Contribution from the Department of Chemistry and Materials Research Center, Northwestern University, Evanston, Illinois 60201

Structure, Conductivity, and Magnetic Properties of (Phthalocyaninato)nickel(II) Bromide

Sharon M. Palmer, Judith L. Stanton, Brian M. Hoffman,* and James A. Ibers*

Received October 11, 1985

The compound (phthalocyaninato)nickel(II) bromide, Ni(pc)Br, has been synthesized by the oxidation of Ni(pc) with Br_2. Comparison of this compound with its isostructural partner Ni(pc)I provides a first glimpse of the effects of change of oxidant on the properties of crystalline porphyrinic molecular metals. Ni(pc)Br, $C_{32}H_{16}BrN_8Ni$, crystallizes with two formula units in space group D_{4h}^2-$P4/mcc$ of the tetragonal system in a cell of dimensions a = 13.793 (7) Å and c = 6.431 (4) Å (167 K). The structure is identical with that of Ni(pc)I and consists of stacks of Ni(pc) molecules segregated from chains of halogen in the form of Br_3^- ions; both stacks and chains run parallel to the c axis of the crystal. Each Ni(pc) molecule is centered on a site of $4/m$ symmetry and is constrained to be planar and perpendicular to the stacking axis. Successive rings in the unit cell are staggered by 39.1 (6)°. Although there is room for about 13% more Br_3^- than I_3^- in such channels, the halogen to Ni(pc) ratio of 1:1 and the degree of oxidation, $^1/_3$ electron/Ni(pc) ring, is the same for both Ni(pc)Br and Ni(pc)I. Despite these structural similarities the electrical conductivity and magnetic properties of Ni(pc)Br ($\sigma \approx 100\ \Omega^{-1}\ cm^{-1}$ at room temperature) differ significantly from those of Ni(pc)I ($\sigma \approx 600\ \Omega^{-1}\ cm^{-1}$ at room temperature), both in value and in temperature variation. Analysis of the EPR measurements suggests that the trihalide chain plays a lesser role in charge transport in Ni(pc)Br and that the Ni(pc) stacks become further decoupled as the temperature is lowered below ca. 75 K. The present results give the first clear evidence that it is inappropriate to ignore anion effects and concentrate on the metal-organic framework in discussions of M(L)X systems.

Introduction

The oxidation by iodine of metallophthalocyanine and -porphyrin compounds has yielded a number of highly conducting compounds.[1-3] The chemical flexibility of these metal-ligand systems permits systematic alterations of their electronic structure through ligand modification and metal substitution. Previous investigations[1b,d,2,3] have included comparisons among a series of compounds Ni(L)I, where the macrocycles L are derivatives of the porphine skeleton. The most extensively characterized compound in this series is (phalocyaninato)nickel(II) iodide, Ni(pc)I,[2] the first low-temperature molecular conductor[2d,e] based on a metal-organic complex. We also compared the effects of metal substitution in the series M(pc)I, where M = Fe,[4] Co,[5] and Cu,[6] in addition to Ni.

Here we report the synthesis, crystal structure, resonance Raman spectroscopy, conductivity behavior, and EPR characteristics of the molecular conductor Ni(pc)Br. Comparison of Ni(pc)Br with its isostructural partner Ni(pc)I provides a first glance of the effects of change of oxidant on the properties of crystalline porphyrinic molecular metals. It provides partial answers to the long-standing question of the factors that determine the compositional structure of the M(L)X compounds and, by inference, other molecular conductors[7] as well. It further provides the first evidence that coupling between M(pc) stacks and X_3^- chains is important to the charge transport process in these materials.

Experimental Section

Synthesis of Ni(pc)Br. (Phthalocyaninato)nickel(II) (Ni(pc)) was purchased from Eastman Kodak Co. and sublimed before use. Single crystals of Ni(pc)Br were prepared in the manner used for Ni(pc)I.[2c] Solid Ni(pc) was placed in one arm of an H-tube filled with 1,2,4-trichlorobenzene solvent, Br_2(l) was added to the other arm, and the tube was sealed. The side containing Ni(pc) was heated to 150-160 °C, and crystals of Ni(pc)Br formed in the cooler portion of the tube. These thin, lustrous, dark green needles generally crystallized in the presence of powder and microcrystalline material, including some unoxidized Ni(pc). Crystals of Ni(pc)Br are very thin needles, the largest being on the order of 1 mm × 0.03 mm × 0.03 mm.

Resonance Raman Spectroscopy. Spectra of microcrystalline samples were recorded at room temperature on a 0.85-m Spex 1401 double monochromator with 5145-Å Ar^+ excitation and a 180° backscattering illumination geometry. The samples were studied in spinning 5-mm Pyrex tubes in order to reduce laser-induced decomposition. The exciting line was used to calibrate spectra.

X-ray Structural Study of Ni(pc)Br. Unit cell parameters of a = 13.793 (7) and c = 6.431 (4) Å at 167 K were determined by least-squares refinement of the setting angles of 13 reflections with $9.5° \leq \theta(\text{Mo K}\alpha_1) \leq 13.0°$ that had been centered on a CAD-4 diffractometer. A preliminary check on intensities suggested Laue group $4/mmm$. Analysis of systematic absences in the final intensity data indicates that the material crystallizes in space group D_{4h}^2—$P4/mcc$, the same space group adopted by the analogous materials M(pc)I (M = Fe,[4] Co,[5] Ni,[2] Cu,[6] and H_2[1d-f]).

Intensity data for the Bragg scattering were collected on the CAD-4 diffractometer at 167 (1) K by the θ-2θ scan technique. No systematic change was observed in the intensities of five standard reflections that were measured every 50 reflections. Data processing and calculations were done by methods standard in this laboratory.[8,9] A value of p = 0.04 was used in the estimation of $\sigma(F^2)$. Experimental details and crystal data are given in Table I.

The starting positional parameters for Ni(pc)Br were those of Ni(pc)I; initially these were refined isotropically. The positions of the H atoms

(1) (a) Ibers, J. A.; Pace, L. J.; Martinsen, J.; Hoffman, B. M. *Struct. Bonding (Berlin)* **1982**, *50*, 1-55. (b) Hoffman, B. M.; Ibers, J. A. *Acc. Chem. Res.* **1983**, *16*, 15-21. (c) Hoffman, B. M.; Martinsen, J.; Pace, L. J.; Ibers, J. A. In *Extended Linear Chain Compounds*; Miller, J. S., Ed.; Plenum: New York, 1983; Vol. 3, pp 459-549. (d) Palmer, S. M.; Stanton, J. L.; Martinsen, J.; Ogawa, M. Y.; Heuer, W. B.; Van Wallendael, S. E.; Hoffman, B. M.; Ibers, J. A. *Mol. Cryst. Liq. Cryst.* **1985**, *125*, 1-11. (e) Palmer, S. M.; Stanton, J. L.; Hoffman, B. M.; Ibers, J. A., unpublished results. (f) Stanton, J. L. Ph.D. Thesis, Northwestern University, **1985**.

(2) (a) Petersen, J. L.; Schramm, C. J.; Stojakovic, D. R.; Hoffman, B. M.; Marks, T. J. *J. Am. Chem. Soc.* **1977**, *99*, 286-288. (b) Schramm, C. J.; Stojakovic, D. R.; Hoffman, B. M.; Marks, T. J. *Science (Washington, D.C.)* **1978**, *200*, 47-48. (c) Schramm, C. J.; Scaringe, R. P.; Stojakovic, D. R.; Hoffman, B. M.; Ibers, J. A.; Marks, T. J. *J. Am. Chem. Soc.* **1980**, *102*, 6702-6713. (d) Martinsen, J.; Greene, R. L.; Palmer, S. M.; Hoffman, B. M. *J. Am. Chem. Soc.* **1983**, *105*, 677-678. (e) Martinsen, J.; Palmer, S. M.; Tanaka, J.; Greene, R. L.; Hoffman, B. M. *Phys. Rev. B: Condens. Matter* **1984**, *30*, 6269-6276.

(3) (a) Phillips, T. E.; Scaringe, R. P.; Hoffman, B. M.; Ibers, J. A. *J. Am. Chem. Soc.* **1980**, *102*, 3435-3444. (b) Martinsen, J.; Pace, L. J.; Phillips, T. E.; Hoffman, B. M.; Ibers, J. A. *J. Am. Chem. Soc.* **1982**, *104*, 83-91.

(4) Palmer, S. M.; Stanton, J. L.; Jaggi, N. K.; Hoffman, B. M.; Ibers, J. A.; Schwartz, L. H. *Inorg. Chem.* **1985**, *24*, 2040-2046.

(5) Martinsen, J.; Stanton, J. L.; Greene, R. L.; Tanaka, J.; Hoffman, B. M., Ibers, J. A. *J. Am. Chem. Soc.* **1985**, *107*, 6915-6920.

(6) Martinsen, J.; Ogawa, M. Y.; Stanton, J. L.; Greene, R. L.; Hoffman, B. M.; Ibers, J. A., manuscript in preparation.

(7) For a review of molecular conductors, see: (a) *Extended Linear Chain Compounds*; Miller, J. S., Ed.; Plenum: New York, 1982. (b) "Proceedings of the International Conference on the Physics and Chemistry of Low-Dimensional Synthetic Metals (ICSM 84)"; *Mol. Cryst. Liq. Cryst.* **1985**, *120*.

(8) Corfield, P. W. R.; Doedens, R. J.; Ibers, J. A. *Inorg. Chem.* **1967**, *6*, 197-204.

(9) See, for example: Waters, J. M.; Ibers, J. A. *Inorg. Chem.* **1977**, *16*, 3273-3277.

0020-1669/86/1325-2296$01.50/0

Table I. Crystal Data and Experimental Details for Ni(pc)Br

compd	Ni(pc)Br
formula	$C_{32}H_{16}BrN_8Ni$
fw	651.15
a,[a] Å	13.793 (7)
c, Å	6.431 (4)
V, Å^3	1224 (2)
Z	2
d_{calcd}, g/cm^3	1.767 at 167 (1) K[b]
space group	D_{4h}^2—$P4/mcc$
cryst shape	needle of square cross section with faces of the forms {100} and {001} having separations of 0.025 mm and 0.377 mm, respectively
cryst vol, mm^3	2.4×10^{-4}
radiation	graphite-monochromated Mo Kα [λ(Kα_1) = 0.7093 Å]
μ, cm^{-1}	24.5
transmissn factors	0.93–0.95
takeoff angle, deg	3.0
receiving aperture, mm	2.0 × 2.0
scan method	ω–2θ
scan speed, deg 2θ/min	2; for reflcns with $I < 3\sigma(I)$ rescans were forced to achieve $I > 3\sigma(I)$, up to 150 s total scan time
scan width, deg	0.5 below Kα_1 to 0.5 above Kα_2
bkgd counts	$^1/_4$° scan on each side of peak
data collcd	$+h,\pm k,+l$ 4° ≤ 2θ ≤ 40°; $+h,+k,+l$ 40° < 2θ ≤ 56°
no. of unique data	812
no. of unique data with $F_o^2 > 3\sigma(F_o^2)$	203
no. of variables in final refin	66
R on F_o^2	0.167
R_w on F_o^2	0.195
R on F_o, $F_o^2 > 3\sigma(F_o^2)$	0.060
R_w on F_o, F_o^2 g $3\sigma(F_o^2)$	0.064
error on observn of unit wt, e^2	0.94

[a] Cell refinement had the imposed constraints $b = a$, $\alpha = \beta = \gamma = 90°$. [b] The low-temperature system is from a desing by Prof. J. J. Bonnet and S. Askenazy and is commercially available from Soterem, Z. I. de Vic, 31320 Castanet-Tolosan, France.

were idealized (C–H = 0.95 Å), and their positions were not varied throughout the remainder of the refinement. Each H atom was given a fixed isotropic thermal parameter 1 Å^2 greater than that of the C atom to which it is attached. In the penultimate cycle of refinement on F_o^2, the occupancy of the Br atom converged to 0.952 (14) per Ni, which we take to be 1.0. Final positional and thermal parameters are listed in Table II. (The atom-labeling scheme is the same as that of Ni(pc)I.[2c]) Table III lists the anisotropic thermal parameters.[10] Table IV lists $10|F_o|$ vs. $10|F_c|$.[10] A negative entry in Table IV signifies $F_o^2 < 0$.

Single-Crystal Electrical Conductivity Studies. Crystals were mounted in integrated circuit cans for ac conductivity measurements as described elsewhere.[2c-e,11] The crystals were mounted on 8-μm graphite fibers[12] and electrical contact was made with a palladium paste.[13] A four-probe low-frequency ac technique, described previously,[11] was utilized to measure sample resistance. Low temperatures were obtained with cold N_2 gas from liquid N_2 boiloff, and the temperature was monitored with a calibrated copper–constantan thermocouple anchored to the sample holder assembly within a few millimeters of the sample. Conductivity was measured along the needle axis (c) of the crystal (the stacking direction). Crystals averaged 1.0 mm in length and 0.02 mm in width. Uncertainty in the crystal dimensions leads to an uncertainty in the absolute conductivity of $\Delta\sigma/\sigma \approx \pm 0.4$.[2c] Relative conductivities, however, are accurate to the level of the resistance measurement (±1%).

Electron Spin Resonance Spectroscopy. Measurements in the range 300–90 K employed a highly modified Varian E-4 X-band EPR spectrometer, with 100 kHz field modulation. Temperatures in this range were obtained by use of cold N_2 gas and a Varian V6040 variable-temperature controller. The sample temperature was monitored with a calibrated copper–constantan thermocouple placed on the sample tube within 5 mm of the sample. Stability was better than ±1 K.

A Varian E-4 spectrometer interfaced to a Varian 9-in. magnet was used to accommodate the cryostat for low-temperature studies. Temperatures down to 5 K were obtained with an Air Products Model LTR liquid-transfer Heli-tran refrigerator in combination with a Scientific Instruments Model 5500-5 microprocessor-based temperature controller. The sample temperature, stable to within ±0.5 K at 100 K and within ±0.2 K at base temperature, was monitored by a calibrated silicon diode cryogenic temperature sensor (Lakeshore Cyrotronics DT-500 DRC).

All EPR experiments were performed on single crystals that were first shown to be highly conductive. The crystal then was removed from its conductivity mount and centered in a notch cut through the solid tip of a sealed quartz tube. The crystal was secured with silicone grease. A temperature sensor was placed inside the tube, positioned in close proximty to the sample, and embedded in silicone grease to ensure thermal contact.

The orientation dependence of the EPR signal was obtained by attaching the sample tube to a goniometer head of standard design mounted to the resonance cavity. Rotation angles were measured to within ±1°. g Values were measured relative to that of DPPH (2,2-diphenyl-1-picrylhydrazyl; $g = 2.0036$) with a Hewlett-Packard Model X5332B frequency meter and a field calibration provided by the spectrum of Mn^{2+} in MgO.

The integrated EPR intensity was obtained by a numerical double integration of the first derivative curve performed on a Fabritek Model 1074 instrumental computer.[2c,e,14]

Table II. Positional Parameters for Ni(pc)Br

atom	x	y	z
Br	1/2	1/2	1/4
Ni	0	0	0
N(1)	0.12399 (67)	0.05901 (75)	0
N(2)	0.08020 (84)	0.22996 (79)	0
C(1)	0.1421 (11)	0.1579 (10)	0
C(2)	0.2472 (10)	0.1736 (10)	0
C(3)	0.30227 (96)	0.2566 (11)	0
C(4)	0.4045 (11)	0.24599 (98)	0
C(5)	0.4449 (10)	0.1551 (11)	0
C(6)	0.39075 (95)	0.0709 (10)	0
C(7)	0.2889 (10)	0.0820 (10)	0
C(8)	0.20915 (90)	0.0148 (11)	0
HlC(3)	0.2738	0.3168	0
HlC(4)	0.4447	0.3018	0
HlC(5)	0.5136	0.1504	0
HlC(6)	0.4182	0.0062	0

Results

Resonance Raman Studies. Resonance Raman spectroscopy was used to determine the form of the bromine species. The only feature in the region 100–650 cm^{-1} is a peak at 161 cm^{-1}, indicative of symmetrical Br_3^-. Free Br_2 (ν = 306 cm^{-1}), Br_5^- (ν = 241 cm^{-1}), and unsymmetrical Br_3^- (ν = 208, 140 cm^{-1})[15] are not present in detectable quantities. By analogy with the study of Ni(pc)I, in which ^{129}I Mössbauer experiments showed that I^- was not present,[2c] we conclude that Ni(pc)Br contains no Br^-. Thus, Br_3^- appears to be the sole halide species present and we formulate this new compound, Ni(pc)Br, as $[Ni(pc)]^{1/3+}$ $(Br_3^-)_{1/3}$.

Description of the Structure of Ni(pc)Br. Ni(pc)Br, Ni(pc)I,[2c] and Co(pc)I[5] are isostructural, and views of the structure are available in ref 2c and 5. The unit cell of Ni(pc)Br, shown in stereo in Figure 1, is composed of stacks of Ni(pc) molecules segregated from chains of Br atoms; both stacks and chains run parallel to the c-axis of the crystal. The bromine chains are located in channels between four stacks of macrocycles. Each Ni(pc) molecule is centered on a site of $4/m$ symmetry and is thus constrained to be planar and perpendicular to the stacking axis.

(10) Supplementary material.
(11) Phillips, T. E.; Anderson, J. R.; Schramm, C. J.; Hoffman, B. M. *Rev. Sci. Instrum.* **1979**, *50* (2), 263–265.
(12) Alfa/Ventron.
(13) Palladium paste is made with palladium powder (0.25–0.55 μm, Alfa/Ventron).
(14) Aasa, R.; Vanngard, T. *J. Magn. Reson.* **1975**, *19*, 308–315.
(15) (a) Kalina, D. W.; Lyding, J. W.; Ratajack, M. T.; Kannewurf, C. R.; Marks, T. J. *J. Am. Chem. Soc.* **1980**, *102*, 7854–7862. (b) Diel, B. N.; Inabe, T.; Lyding, J. W.; Schoch, K. F., Jr.; Kannewurf, C. R.; Marks, T. J. *J. Am. Chem. Soc.* **1983**, *105*, 1551–1567.

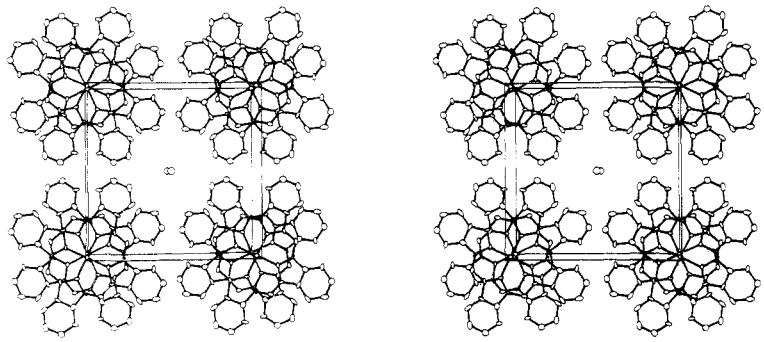

Figure 1. Stereoview down the *c* axis of Ni(pc)Br.

Table V. Bond Distances (Å) and Angles (deg) for Ni(pc)Br

Ni–N(1)	1.89 (1)	C(2)–C(3)	1.37 (2)
N(1)–C(1)	1.39 (2)	C(2)–C(7)	1.39 (2)
N(1)–C(8)	1.32 (2)	C(3)–C(4)	1.42 (2)
N(2)–C(1)	1.31 (2)	C(4)–C(5)	1.37 (2)
N(2)–C(8)	1.34 (2)	C(5)–C(6)	1.38 (2)
C(1)–C(2)	1.47 (2)	C(6)–C(7)	1.41 (2)
N(1)–Ni–N(1′)	90.0	C(7)–C(8)	1.44 (2)
C(1)–N(1)–C(8)	107 (1)	C(3)–C(4)–C(5)	120 (1)
C(1)–N(2)–C(8)	118 (1)	C(4)–C(5)–C(6)	123 (1)
N(1)–C(1)–N(2)	129 (1)	C(5)–C(6)–C(7)	117 (1)
N(1)–C(1)–C(2)	109 (1)	C(2)–C(7)–C(6)	121 (1)
N(2)–C(1)–C(2)	122 (1)	C(2)–C(7)–C(8)	106 (1)
C(1)–C(2)–C(3)	132 (1)	C(6)–C(7)–C(8)	134 (1)
C(1)–C(2)–C(7)	106 (1)	N(1)–C(8)–N(2)	130 (1)
C(3)–C(2)–C(7)	122 (1)	N(1)–C(8)–C(7)	112 (1)
C(2)–C(3)–C(4)	118 (1)	N(2)–C(8)–C(7)	118 (1)

Successive rings in the unit cell are staggered by 39.1 (6)°.

Raman spectra of Ni(pc)Br indicate the presence of symmetric Br_3^- and the absence of Br_2, Br_5^-, and asymmetric Br_3^-. The model for I disorder in Ni(pc)I is that of ordered chains of I_3^- ions that are disordered with respect to neighboring chains.[2c] This model is based on an analysis of diffuse X-ray scattering. The manifestation in the Bragg scattering of this disorder is the large apparent thermal motion of the I atom in the chain direction. Such apparent motion is also observed (Table III) in the present compound, Ni(pc)Br. In fact, the ratio of the thermal amplitude along the chain, $U_{\parallel}$, to that perpendicular to the chain, $U_{\perp}$, is 3.59 for Br in Ni(pc)Br, while $U_{\parallel}/U_{\perp}$ is 1.42 for I in Ni(pc)I. Owing to the smaller size of the Br atom compared with I there is more room for the symmetric Br_3^- ion to "rattle" in the chain direction; presumably this leads to positional disorder *within* a halide chain, and hence the larger apparent thermal motion. But given the fact that the Br_3^- ion is substantially smaller than the I_3^- ion it is especially significant that in each instance the final composition is $Ni(pc)(X_3)_{1/3}$; this indicates the overriding importance of electronic factors, since the structure clearly could have accommodated additional Br_3^- ions. A rough estimate of the discrepancy can be made as follows: The Br–Br spacing within the symmetric Br_3^- ion can be taken as 2.55 Å.[16] The Br···Br distance between ions in a chain of Br^{3-} ions can be estimated as 3.44 Å from the $Br_5SbBr\cdots Br_3^-$ distance,[17] in agreement with considerations based on the relative van der Waals radii of Br^- and I^-. This leads to an expected repeat distance within the Br_3^- chain of 8.54 Å, compared with the repeat distance of 9.72 Å for I_3^- chains in M(pc)I. If this expectation had been realized, Br_2 oxidation of Ni(pc) would have produced the compound $Ni(pc)Br_{1.13}$ rather than the observed compound $Ni(pc)Br_{1.0}$.

Bond parameters of the Ni(pc) ring in Ni(pc)Br are listed in Table V. There are no major differences in bond lengths or angles from those of Ni(pc) in Ni(pc)I. The numbering scheme is that used for Ni(pc)I.[2c]

(16) See, for example: Lawton, S. L.; McAfee, E. R.; Benson, J. E.; Jacobson, R. A. *Inorg. Chem.* **1973**, *12*, 2939–2944.
(17) Lawton, S. L.; Hoh, D. M.; Johnson, R. C.; Knisely, A. S. *Inorg. Chem.* **1973**, *12*, 277–283.

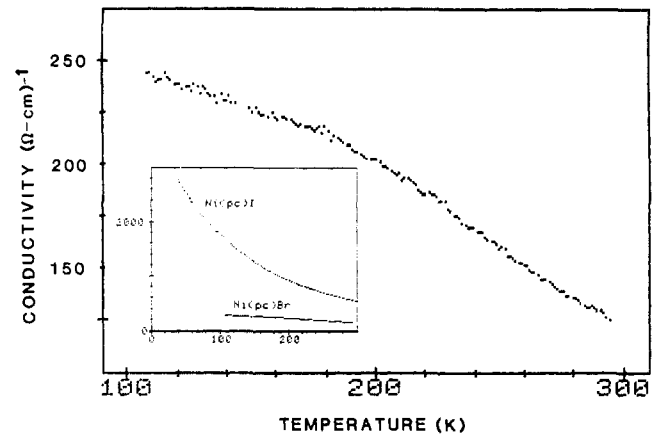

Figure 2. Temperature response of the conductivity along the needle (*c*) axis of a single crystal of Ni(pc)Br. Inset: Comparison between the conductivities of Ni(pc)Br and Ni(pc)I.

Conductivity Measurements. The conductivity along the *c* axis of single crystals of Ni(pc)Br is high at room temperature, ranging from 125 to 200 Ω^{-1} cm^{-1}. Despite large experimental uncertainty in the absolute value of $\sigma_{\parallel}$, the value for Ni(pc)Br clearly is approximately half that for Ni(pc)I. Figure 2 presents conductivity data as a function of temperature. For all crystals measured, the conductivity increases smoothly as the temperature is lowered from room temperature down to 180–200 K, reaching a value about 1.8 times that at room temperature. The conductivity continues to rise as the temperature is lowered, but at a slower rate. All crystals studied to date have shown a sharp, irreversible loss in conductivity at some temperature below about 100 K. This decline arises from stresses on the very fragile crystals as the result of cooling. However, the behavior above 100 K is reproducible and reversible and thus represents the intrinsic conductivity of Ni(pc)Br.

The first portion of the conductivity curve of Ni(pc)Br, the smooth rise for $200 < T < 300$ K, may be fit to the expression

$$\frac{\rho(T)}{\rho(T_1)} = a + b\left(\frac{T}{T_1}\right)^{\gamma} \qquad (1)$$

with $\gamma = 1.45$–1.5. The same fit yields a similar value, $\gamma = 1.7$, for Ni(pc)I.[2e] Both values are higher than observed for simple metals ($\gamma = 1$) and less than the typical values for organic conductors ($\gamma = 2$–2.4).

Why the conductivity of Ni(pc)Br, as opposed to that of Ni(pc)I, begins to level off below 200 K we do not understand; however, the EPR characteristics of Ni(pc)Br and Ni(pc)I begin to differ in this region as well (vide infra).

Electron Spin Resonance Measurements. Spectra of Ni(pc)Br single crystals show a single resonance whose integrated intensity is independent of temperature from room temperature down to 4 K, indicative of Pauli paramagnetism (Figure 3). The absolute value of the magnetic susceptibility has not been determined because pure Ni(pc)Br is not available in sufficient quantities. However, the intensity of the signal from a single crystal of

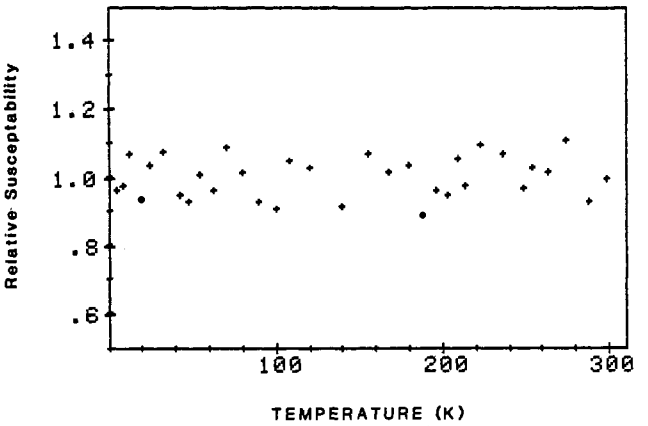

Figure 3. Temperature dependence of the single-crystal EPR spin susceptibility of Ni(pc)Br, normalized to the room-temperature value.

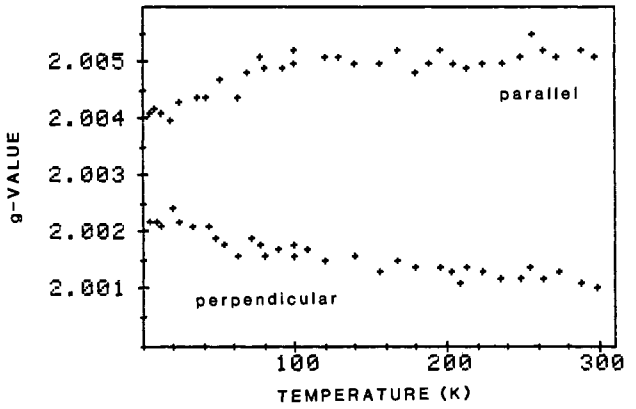

Figure 4. Temperature dependence of the g-tensor components of Ni(pc)Br.

Ni(pc)Br is comparable with that of a crystal of Ni(pc)I of similar size under the same conditions. Thus, the value of χ^s for Ni(pc)I, 2.01 emu/mol,[2c,e] may be taken as a reasonable estimate of χ^s for Ni(pc)Br. Since the bandwidth of a molecular conductor is inversely related to the Pauli susceptibility, the conclusion that the isostructural and isoionic Ni(pc)I and Ni(pc)Br compounds have comparable susceptibilities implies that they have comparable bandwidths.

***g* Values.** The g tensor of Ni(pc)Br has axial symmetry; the unique axis of the g tensor corresponds to the needle axis of the crystal (the *c* axis) and is designated the parallel direction. The *g* values can be fit to eq 2, where θ is the angle between the applied

$$g(\theta) = [g_\parallel^2 \cos^2\theta + g_\perp^2 \sin^2\theta]^{1/2} \qquad (2)$$

magnetic field H_0 and the *c* axis. At ambient temperature $g_\parallel$ = 2.0051 and $g_\perp$ = 2.0011.

These *g* values, which are so near to the free-electron value, show that the oxidation is ligand-centered, as has been demonstrated for Ni(pc)I.[2] A metal-centered oxidation would result in *g* values similar to those determined for $[Ni^{III}(pc)]^+$,[18] $g_\perp$ = 2.29 and $g_\parallel$ = 2.11. However, for a π-cation radical species one would expect to find $g_\parallel \sim g_\perp \sim g_e$, but with $g_\perp > g_\parallel$. The observed inequality, $g_\parallel > g_\perp \approx g_e$, was interpreted for Ni(pc)I as evidence for weak coupling between Ni(pc) stacks and I_3^- chains with back charge transfer from an I_3^- ion to a macrocyclic stack,[2c] and a similar analysis can be applied to Ni(pc)Br. This is represented by the simple Mulliken charge-transfer wave function[2c,3a]

$$|\Psi\rangle = (1-\alpha^2)^{1/2}|(Ni(pc))_3^+(Br_3)^-\rangle + \alpha|(Ni(pc))_3(Br_3)^\bullet\rangle$$

where α^2 is the degree of back charge transfer from Br_3^- to the partially oxidized macrocycle. This leads to the following formulas

(18) Bobrovskii, A. P.; Sidorov, A. N. *J. Struct. Chem. (Engl. Transl.)* **1976**, *17*, 50–54.

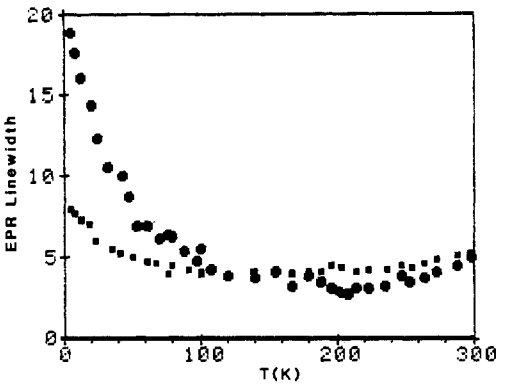

Figure 5. Temperature dependence of the EPR line widths of Ni(pc)Br with the magnetic field parallel (■) and perpendicular (●) to the needle (*c*) axis.

Table VI. Crystal Structure Data for M(pc)X Compounds

compd	M–M, Å		*T*, K
	interstack	intrastack	
Ni(pc)I[a]	13.94 (1)	3.244 (2)	298
Ni(pc)Br[b]	13.79 (1)	3.216 (2)	167
H_2(pc)I[c]	13.91 (2)	3.205 (5)	97
Fe(pc)I[d]	13.84 (2)	3.39 (1)	97
Co(pc)I[e]	13.93 (1)	3.123 (1)	116
Cu(pc)I[f]	13.89 (1)	3.195 (4)	97

[a] Reference 2c. [b] This work. [c] Reference 1d–f. [d] Reference 4. [e] Reference 5. [f] Reference 6.

for the components of the g tensor with respect to the ligand-centered oxidation:

$$g_\parallel \sim g_e + 2\alpha^2 \qquad g_\perp \sim g_e \qquad (3)$$

The observed value of $g_\parallel$ yields α^2 = 0.001, half that in Ni(pc)I.

The *g* values are roughly temperature-independent, or at most slightly temperature-dependent above $T \sim 75$ K (Figure 4). However, as the temperature is decreased from 75 K, $g_\parallel$ unexpectedly begins to decrease and there may be an accompanying slight increase in $g_\perp$, although the latter change is near the limits of error. From eq 3 the decrease in $g_\parallel$ reflects a loss of back-bonding to the Br_3^- chain upon cooling below 75 K, an effect that is not seen with Ni(pc)I.

Line Widths. The EPR line for Ni(pc)Br is narrow with a symmetric and roughly Lorentzian line shape. At room temperature the width is approximately isotropic, $\Gamma_\parallel \sim \Gamma_\perp \sim$ 4–5 G, and its magnitude is characteristic of a π radical. Both $\Gamma_\parallel$ and $\Gamma_\perp$ decrease slightly upon cooling from 300 to 200 K, and remain essentially constant as the temperature is further lowered from 200 to 100 K (Figure 5). In this temperature range the conductivity of Ni(pc)Br is metal-like; this initial decrease in line width parallels the behavior of Ni(pc)I and is suggestive of increased motional narrowing as the carrier mobility increases upon cooling.

Below 100 K the line width of Ni(pc)Br increases markedly with decreasing temperature. Because $\Gamma_\perp$ experiences a larger increase, the width becomes increasingly anisotropic. Thus the line widths, even more clearly than the *g* values, indicate that the properties of the Ni(pc)Br carrier spins change significantly at temperatures below ca. 100 K. The behavior contrasts sharply with that of Ni(pc)I, where the anisotropy in the line width first decreases as the temperature is lowered and then remains constant with further cooling. Unfortunately, measurements of the Ni(pc)Br conductivity below 100 K have not been possible and the line width and conductivity cannot be correlated at those temperatures.

Discussion

The molecular conductor Ni(pc)Br is isostructural with the M(pc)I series (M = Fe, Co, Ni, Cu, and "H_2").[1d] The intrastack spacing is ca. 3.23 Å in all the M(pc)X compounds where charge transport is ligand-based (Ni(pc)Br; M(pc)I, M = Ni, Cu, and

H_2), but this spacing does vary with the nature of the partial oxidation of the M(pc) rings (Table VI). For example in Co(pc)I partial oxidation occurs at the metal center rather than the ring, and the compound thus is a metal-spine conductor. Bonding interactions between partially oxidized $Co^{2.33}$ centers in Co(pc)I substantially shorten the Co–Co distance to 3.123 (1) Å.[5]

Although Br atoms are smaller and Br_3^- chains shorter than their iodine analogues, the intrastack spacing in Ni(pc)Br is no shorter than that of Ni(pc)I. Viewed another way, there is room for ca. 13% more Br_3^- than I_3^- in the channels between phthalocyanine stacks. Since Br_2 is a stronger oxidant than I_2, further oxidation of the Ni(pc) system is favored. Yet the halogen to Ni(pc) ratio of 1:1 and the degree of oxidation, $^1/_3$ electron/Ni(pc) ring, are the same for oxidation by Br_2 and I_2. Thus the size and structure of the counterion do not determine the degree of oxidation, but rather it appears that the degree of charge transfer is largely a function of the crystal structure as dictated by the donor units. This finding is in accord with other studies[19] of metallophthalocyanine donors in combination with various dopants of different sizes and structures, such as TCNQ, DDQ, BF_4^-, and PF_6^-,[20] where the maximum dopant level is invariably $\sim^1/_3$. However, these studies are complicated by problems of inhomogeneous doping. Euler[21] has suggested that the rotation angle between adjacent phthalocyanine rings is determined by the size of the counterion and that the angle will constrict to ~35° for Ni(pc)Br.[22] However, the rotation angle of 40° between adjacent phthalocyanine rings in M(pc)I compunds remains unchanged in Ni(pc)Br. In short the metrical properties of M(pc)X are insensitive to the form of the counterion.

Despite the structural similarities, the conductivity and magnetic properties of Ni(pc)Br differ significantly from those of Ni(pc)I. The conductivity of the former increases upon cooling from room temperature, but then appears to level off by ca. 100 K, whereas that of the latter continues to increase down to at least 20 K, and remains high down to ~50 mK. Analysis of the carrier–spin g values suggests that the trihalide chain plays a lesser role in charge transport in Ni(pc)Br. More unusual, the analysis indicates that the Ni(pc) stacks become further decoupled as the temperature is lowered below ca. 75 K. The decoupling is accompanied by line width increases, which suggests that it reduces the mobility of the carrier spins. In contrast Ni(pc)I exhibits temperature-independent g values and the line width does not show the low-temperature increase seen in Figure 5 for Ni(pc)Br.

The physical basis for this decoupling and apparent loss of three-dimensional interaction in Ni(pc)Br will be characterized by low-temperature structural and NMR relaxation studies. However, the present results give the first clear evidence that it is inappropriate to ignore anion effects and concentrate on the metal–organic framework in discussions of the M(L)X systems.

Acknowledgment. This work was supported by the Northwestern University Materials Research Center under the National Science Foundation NSF-MRL program (Grant DMR 82-16972) and through the Solid State Chemistry Program of the National Science Foundation (Grant DMR 81-16804 to B.M.H.).

Registry No. Ni(pc), 14055-02-8; Br_2, 7726-95-6; Ni(pc)Br, 97187-14-9.

Supplementary Material Available: Table III, anisotropic thermal parameters (1 page). Ordering information is given on any current masthead page.

(19) Inabe, T.; Kannewurf, C. R.; Lyding, J. W.; Moguel, M. K.; Marks, T. J. *Mol. Cryst. Liq. Cryst.* **1983**, *93*, 355–367.
(20) DDQ = 2,3-dichloro-5,6-dicyano-1,4-benzoquinone; TNCQ = 7,7,8,8-tetracyano-*p*-quinodimethane.
(21) Euler, W. B. *Inorg. Chem.* **1984**, *23*, 2645–2650.
(22) Neither the Madelung energy (ref 21) nor the EHMO (ref 23) calculations account for the observed rotation angles.
(23) (a) Whangbo, M.-H.; Stewart, K. R. *Isr. J. Chem.* **1983**, *23*, 133–138. (b) Canadell, E.; Alvarez, S. *Inorg. Chem.* **1984**, *23*, 573–579.

Contribution from the Department of Chemistry, University of New Orleans, New Orleans, Louisiana 70148, and Laboratoire de Spectrochimie des Elements de Transition, Université de Paris-Sud, 91405 Orsay, France

Binuclear Molecules Incorporating Small Molecules as Bridging Ligands. Magnetic Properties and Molecular Structure of $[Cu_2L(\mu\text{-}B)]^{2+}$ Where B = OH^- or Br^- and HL = 2,6-Bis(*N*-(2-pyridylmethyl)formidoyl)-4-methylphenol

Charles J. O'Connor,*[1a,b] Dale Firmin,[1a] Arun K. Pant,[1a,2] B. Ram Babu,[1a] and Edwin D. Stevens[1a]

Received January 15, 1986

The syntheses, crystal structures, and magnetic properties are reported for a series of copper(II) complexes prepared from a five-coordinate binucleating ligand, L^-, where HL = 2,6-bis(*N*-(2-pyridylmethyl)formidoyl)-4-methylphenol. These complexes incorporate different small exogenous ions (B^-) into a bridging position to form copper(II) *binuclear* complexes of the formula $[Cu_2L(B)]^{2+}$, and the various degrees of antiferromagnetic coupling are reported. Crystal data: $[Cu_2L(OH)](ClO_4)_2$, monoclinic, space group $P2_1/n$, $Z = 4$, $a = 21.167$ (4) Å, $b = 8.836$ (4) Å, $c = 13.834$ (3) Å, $\beta = 109.22$ (2)°, $V = 2443$ Å^3, $R = 3.3\%$ for 3723 reflections; $[Cu_2L(Br)]Br_2$, triclinic, space group $P\bar{1}$, $Z = 2$, $a = 7.601$ (7) Å, $b = 11.456$ (4) Å, $c = 13.266$ (8) Å, $\alpha = 77.10$ (4)°, $\beta = 83.88$ (6)°, $\gamma = 76.67$ (4)°, $V = 1094$ Å^3, $R = 5.9\%$ for 2544 reflections; $[Cu_2L(OH)](NO_3)_2 \cdot H_2O$, monoclinic, space group Pn, $Z = 2$, $a = 7.438$ (2) Å, $b = 14.823$ (2) Å, $c = 10.399$ (4) Å, $\beta = 90.23$ (2)°, $V = 1147$ Å^3, $R = 2.5\%$ for 2024 reflections.

Introduction

Magnetic interactions in binuclear complexes continue to be an area of research actively pursued by many laboratories. Over the past few years, the emphasis has shifted from the purely magnetic interest in exchange coupling to magnetostructural correlations in exchange-coupled systems.[3,4] From the literature of magnetochemical studies of binuclear complexes, it has become evident that metal complexes prepared from binucleating ligands

(1) (a) University of New Orleans. (b) Université de Paris-Sud.
(2) Permanent address: Department of Physics, University of Gorakhpur, Gorakhpur 273001, India.
(3) Willette, R. D., Gatteschi, D., Kahn, O., Eds. *Magneto-Structural Correlations in Exchange Coupled Systems*; D. Reidel: Dordrecht, Holland, 1984.
(4) O'Connor, C. J. *Prog. Inorg. Chem.* **1982**, *29*, 203.

0020-1669/86/1325-2300$01.50/0